J. Am. Chem. Soc. 1988, 110, 5471-5479

Catalytic Photochemical Oxidation of Organic Substrates by Polyoxometalates. Picosecond Spectroscopy, Photochemistry, and Structural Properties of Charge-Transfer Complexes between Heteropolytungstic Acids and Dipolar Organic Compounds

Craig L. Hill,[*,†] **Donald A. Bouchard,**[†] **Miryam Kadkhodayan,**[†] **Michael M. Williamson,**[†] **Jeffrey A. Schmidt,**[‡] **and Edwin F. Hilinski**[*,‡]

Contribution from the Department of Chemistry, Emory University, Atlanta, Georgia 30322, and Department of Chemistry, The Florida State University, Tallahassee, Florida 32306.
Received November 16, 1987

Abstract: The chemical and photochemical characteristics of hydrated heteropolytungstic acids of the Keggin (T_d) structure, dissolved in three representative dipolar aprotic organic media (DP), *N*-methylpyrrolidinone (NMP), 1,1,3,3-tetramethylurea (TMU), and 1,3-dimethyl-2-imidazolidinone (DMEU), have been investigated. The photochemical and spectroscopic behavior of heteropoly complexes is qualitatively different in these solvents relative to the media conventionally used in polyoxometalate investigations (water, alcohols, acetonitrile, etc.). When the hydrated heteropoly acid α-$H_3PW_{12}O_{40}$ dissolves in NMP, TMU, or DMEU, crystalline complexes of the formula $[(DP)_2H]_3[\alpha\text{-}PW_{12}O_{40}]$ (**1**–DP), where DP = NMP, TMU, and DMEU, can be isolated. Both the solutions and crystals of these salts are colored unlike the component chromophores DP or α-$PW_{12}O_{40}^{3-}$ alone, and irradiation of either the solutions or the crystals results in reduction of the α-$PW_{12}O_{40}^{3-}$ and oxidation of the DP. Although **1**–DP complexes generally crystallize in a disordered manner, disorder-free crystals of one complex, **1**–TMU, were obtained: monoclinic $C2/c$, with a = 21.3221 (87) Å, b = 13.8654 (47) Å, c = 24.8262 (71) Å, β = 100.830 (28)°, V = 7208.87 (4.23) Å^3, and Z = 4; final R = 0.0387 (R_w = 0.0324). The pronounced and photosensitive chromophore in the visible region of **1**–TMU does not derive from covalent or hydrogen-bonding interactions between the organic $[(TMU)_2H]^+$ ions and the inorganic polyoxometalate anion. Characterization of solutions of **1**–DP in acetonitrile and in DP by ^{1}H, ^{17}O, ^{31}P, and ^{183}W NMR and electronic absorption spectroscopy establish that the formation of the intermolecular electron donor–acceptor species can be a reversible process in solution. The kinetics for the photochemical production of the reduced heteropolytungstate products (one-electron heteropoly blue) have been examined under several conditions. A general feature of this photoredox chemistry is fairly constant quantum yields throughout the low-energy region of the absorption spectrum for any given system. The quantum yields at 320 nm for **1**–TMU in TMU and **1**–DMEU in DMEU are 0.27 and 0.17, respectively. The above physical, chemical, and photochemical properties of the **1**–DP in DP systems define appropriate conditions for picosecond spectroscopic examination of polyoxometalate photochemical processes. The evolution of absorption spectral transients on the picosecond timescale with 355-nm laser excitation of the **1**–NMP in NMP and **1**–DMEU in DMEU indicates that two or more distinct species are formed on a time scale (<80 ps) faster than bimolecular diffusion, one within the laser pulse (<20 ps). The picosecond spectroscopy of the above systems is distinct from that observed for α-$H_3PW_{12}O_{40}\cdot nH_2O$, n = 7, in acetonitrile excited at 355 nm. Picosecond spectroscopic control experiments with tetracyanoethylene (TCNE) and NMP indicate that TCNE anion radical and NMP cation radical are produced in <25 ps. The chromophore of NMP cation radical cannot be observed under the conditions used in the **1**–DP/DP picosecond experiments. This work indicates that key photophysical events associated with **1**–DP take place on the subnanosecond timescale.

Heteropoly acids and other polyoxometalates of the early transition metals have attracted much recent attention as soluble and experimentally tractable analogues of metal oxide surfaces.[1,2] Representatives of this large and diverse class of inorganic complexes have been used as catalysts for both homogeneous[3] and heterogeneous[4] processes and used to model metal oxide supported organometallic species.[5-8] In addition, a sizable number of investigations in the last few years have addressed the photophysical and photochemical properties of polyoxometalates.[9-21] In particular, the use of polyoxometalates as catalysts for photochemical and photosynthetic processes involving organic substrates has developed rapidly. The latter processes are some of the most complex homogeneous redox processes in the literature.[10-14,16-21]

Our interest in the systems constituted by heteropolytungstates in dipolar aprotic organic media, examined in detail here, is 3-fold. First, these systems provide the potential for moving catalytic polyoxometalate-based photochemical processes from the near-UV into the visible region of the spectrum, based on our current knowledge of polyoxometalate photoinduced redox processes.[17,19] The ability of many isopoly and heteropoly compounds to photooxidize organic substrates, SH_2, upon irradiation (as exemplified with the complex α-$PW_{12}O_{40}^{3-}$ in the eq 1–3) is well-

$$\alpha\text{-}PW_{12}O_{40}^{3-} + h\nu \rightarrow \alpha\text{-}PW_{12}O_{40}^{3-*} \tag{1}$$

$$\alpha\text{-}PW_{12}O_{40}^{3-*} + SH_2 \rightarrow \alpha\text{-}PW_{12}O_{40}^{4-} + {}^{\bullet}SH + H^+ \tag{2}$$

$$\alpha\text{-}PW_{12}O_{40}^{3-} + {}^{\bullet}SH \rightarrow \alpha\text{-}PW_{12}O_{40}^{4-} + S + H^+ \tag{3}$$

P = heteropoly or isopolyoxometalate catalyst, SH_2 =
one of many organic substrates

known.[10-14,16-21] The resulting reduced polyoxometalates, most

---

[†] Emory University.

[‡] The Florida State University.

(1) Pope, M. T. *Heteropoly and Isopoly Oxometalates*; Springer-Verlag: Berlin, 1983.

(2) Day, V. W.; Klemperer, W. G. *Science (Washington, D.C.)* **1985**, *228*, 533.

(3) Reviews: (a) Kozhevnikov, I. V.; Matveev, K. I. *Russ. Chem. Rev. (Engl. Transl.)* **1982**, *51*, 1075. (b) Kozhevnikov, I. V.; Matveev, K. I. *Appl. Catal.* **1983**, *5*, 135.

(4) A large number of papers addressing the use of polyoxometalates in heterogeneous catalysis exist. Recent representative examples: (a) McMonagle, J. B.; Moffat, J. B. *J. Catal.* **1985**, *91*, 132. (b) Moffat, J. B. *J. Mol. Catal.* **1984**, *26*, 385. (c) Akimoto, M.; Ikeda, H.; Okabe, A.; Echigoya, E. *J. Catal.* **1984**, *89*, 196. (d) Hayashi, H.; Moffat, J. B. *Ibid.* **1983**, *83*, 192; *81*, 61. (e) Konshi, Y.; Sakata, K.; Misono, M.; Yoneda, Y. *Ibid.* **1982**, *77*, 169.

0002-7863/88/1510-5471$01.50/0

commonly referred to as heteropoly blue (HPB) compounds, are, in many cases, readily reoxidized, either by reaction with O_2 (eq 4) or with H^+ (eq 5), to regenerate the oxidized polyoxometalates.

$$2\alpha\text{-}PW_{12}O_{40}{}^{4-} + 2H^+ + {}^1/{}_2O_2 \rightarrow 2\alpha\text{-}PW_{12}O_{40}{}^{3-} + H_2O \quad (4)$$

$$\alpha\text{-}PW_{12}O_{40}{}^{4-} + H^+ \rightarrow \alpha\text{-}PW_{12}O_{40}{}^{3-} + {}^1/{}_2H_2 \quad (5)$$

The reduced polyoxometalate reoxidation processes (eq 4 or 5) define two families of cycles based on polyoxometalates for the homogeneous catalytic photochemical oxidation and dehydrogenation of organic substrates (eq 6 and 7, respectively).[10-21] In

$$SH_2 + {}^1/{}_2O_2 + h\nu \xrightarrow{\alpha\text{-}PW_{12}O_{40}{}^{3-}} S + H_2O \quad (6)$$

$$SH_2 + h\nu \xrightarrow{\alpha\text{-}PW_{12}O_{40}{}^{3-}} S + H_2 \quad (7)$$

the conventional solvents, water, alcohols, and acetonitrile, used for a great majority of the polyoxometalate investigations, the photochemical action spectra for eq 1–3 and the electronic adsorption spectra of the polyoxometalates are principally in the ultraviolet. In contrast, many polyoxometalates form highly photosensitive solutions in a number of dipolar aprotic organic media, and the absorption and photochemical action spectra of these systems, including the catalytically effective tungstates, can shift into the visible by hundreds of nanometers.[17,19,22] These solvent-induced shifts can increase overlap of the polyoxometalate spectra with the solar spectrum by a factor of 21, relative to water or acetonitrile solutions, warranting an examination of the molecular origins of such solvent-induced shifts. Our second interest in the systems reported here derives from the interesting and unusual characteristics of polyoxometalate-based photochemical processes involving organic substrates. The production of C–C and C–N bonds from saturated hydrocarbon C–H bonds are two examples.[18]

The third impetus for this research derives from the ability to isolate crystalline, experimentally tractable complexes formed between the dipolar aprotic organic molecules (DP) and the polyoxometalates that retain the high susceptibilities (quantum yields 0.1–0.15 or higher) to photoinduced redox processes (eq 1–3).[19,20] These systems may help model and thus probe some of the electronic and other features displayed by the metal oxide–liquid interface, including features of irradiated semiconductor metal oxides surfaces in contact with organic liquids. To date, photosensitive complexes between heteropolymolybdic acids of the T_d Keggin structure and two dipolar aprotic organic compounds 1,1,3,3-tetramethylurea (TMU)[19] and *N*,*N*-dimethylacetamide (DMA)[20] have been isolated and characterized. However, the corresponding photosensitive complexes involving the catalytically more effective heteropolytungstates have proven to be less amenable to experimental manipulation.

This paper reports characterization of the photochemically active systems constituted by the heteropolytungstic acid α-$H_3PW_{12}O_{40}$ (**1**) dissolved in the dipolar aprotic organic media, *N*-methylpyrrolidinone (NMP), 1,1,3,3-tetramethylurea, and 1,3-dimethyl-2-imidazolidinone (common name dimethylethyleneurea or DMEU). The properties of these solutions are examined by ^{1}H, ^{17}O, ^{31}P, and ^{183}W NMR and electronic absorption spectroscopy. An X-ray crystal structure of one orange photosensitive complex between α-$H_3PW_{12}O_{40}$ and TMU, $[(TMU)_2H]_3[\alpha\text{-}PW_{12}O_{40}]$ (**1**-TMU), is reported. These studies collectively provide the necessary background for examination of the electronic absorption spectral characteristics of the **1**–NMP and **1**–DMEU systems on the critical picosecond time scale.[23] Although a number of flash photolysis studies on polyoxometalate systems on the microsecond and slower time scales have now been reported, generation of the charge-transfer excited states as well as the actual intermolecular redox event(s) themselves appears to be over within the lifetime of the flash in all these studies.[10,12,13] The work in this paper indicates that key photophysical events in DP–polyoxometalate photochemistry occur in times far shorter than 1 ns.

Experimental Section

Materials. The solvents and the dipolar organic substrate *N*-methylpyrrolidinone were Burdick and Jackson glass-distilled grade and were used as received. The dipolar organic substrates 1,1,3,3-tetramethylurea and 1,3-dimethyl-2-imidazolidinone were reagent grade from Aldrich and were used without further purification. Water isotopically enriched in ^{17}O was purchased from Department of Energy/Monsanto. The reactant α-$H_3PW_{12}O_{40}\cdot nH_2O$ was prepared by literature procedures.[24] Hygroscopic organic solvents were stored in Aldrich Sure-Seal bottles or in Schlenk flasks and were manipulated under argon. The light-sensitive complexes, $[(DP)_2H]_3[PW_{12}O_{40}]$ (**1**-DP), where DP = NMP, TMU, or DMEU, were stored in amber wide-mouth bottles and kept out of direct room light at all times. As the hydrated heteropolytungstic acids, and to a lesser extent the product electron donor–acceptor

---

(5) (a) Besecker, C. J.; Klemperer, W. G. *J. Organomet. Chem.* **1981**, *205*, C31. (b) Besecker, C. J.; Day, V. W.; Klemperer, W. G.; Thompson, M. R. *J. Am. Chem. Soc.* **1984**, *106*, 4125. (c) Besecker, C. J.; Day, V. W.; Klemperer, W. G.; Thompson, M. R. *Inorg. Chem.* **1985**, *24*, 44. (d) Day, V. W.; Klemperer, W. G.; Maltbie, D. J. *Organometallics* **1985**, *4*, 104. (e) Besecker, C. J.; Klemperer, W. G.; Maltbie, D. J.; Wright, D. A. *Inorg. Chem.* **1985**, *24*, 1027. (f) Che, T. M.; Day, V. W.; Francesconi, L. C.; Fredrich, M. F.; Klemperer, W. G. *Ibid.* **1985**, *24*, 4055. (g) Day, V. W.; Earley, C. W.; Klemperer, W. G.; Maltbie, D. J. *J. Am. Chem. Soc.* **1985**, *107*, 8261 and references cited in each.

(6) (a) Finke, R. G.; Droege, M.; Hutchinson, J. R.; Gansow, O. *J. Am. Chem. Soc.* **1981**, *103*, 1587. (b) Finke, R. G.; Droege, M. W. *Ibid.* **1984**, *106*, 7274. (c) Finke, R. G.; Droege, M. W.; Cook, J. C.; Suslick, K. S. *Ibid.* **1984**, *106*, 5750 and references in each.

(7) (a) Reference 1, Chapter 7. (b) Zonnevijlle, F.; Pope, M. T. *J. Am. Chem. Soc.* **1979**, *101*, 2731.

(8) (a) Knoth, W. H. *J. Am. Chem. Soc.* **1979**, *101*, 759. (b) Knoth, W. H. *Ibid.* **1979**, *101*, 2211. (c) Domaille, P. J.; Knoth, W. H. *Inorg. Chem.* **1983**, *22*, 818. (d) Knoth, W. H.; Domaille, P. J.; Farlee, R. D. *Organometallics* **1985**, *4*, 62.

(9) (a) Yamase, T. *Chem. Lett.* **1973**, 615. (b) Yamase, T.; Hayashi, H.; Ikawa, T. *Ibid.* **1974**, 1055. (c) Yamase, T.; Ikawa, T. *Bull. Chem. Soc. Jpn.* **1977**, *50*, 746. (d) Yamase, T. *J. Chem. Soc., Dalton Trans.* **1978**, 238. (e) Yamase, T.; Ikawa, T. *Inorg. Chim. Acta* **1979**, *37*, L529. (f) Yamase, T.; Ikawa, T. *Ibid.* **1980**, *45*, L55. (g) Yamase, T. *Ibid.* **1981**, *54*, L165. (h) Yamase, T.; Sasaki, R.; Ikawa, T. *J. Chem. Soc., Dalton Trans.* **1981**, 628. (i) Yamase, T. *Inorg. Chim. Acta* **1981**, *54*, L207. (j) Yamase, T. *Ibid.* **1982**, *64*, L155. (k) Yamase, T. *J. Chem. Soc., Dalton Trans.* **1982**, 1987. (l) Yamase, T.; Kurozumi, T. *Ibid.* **1983**, 2205. (m) Yamase, T. *Inorg. Chim. Acta* **1983**, *76*, L25. (n) Yamase, T.; Kurozumi, T. *Ibid.* **1984**, *83*, L25. (o) Yamase, T. *J. Chem. Soc., Dalton Trans.* **1985**, 2586.

(10) (a) Yamase, T.; Takabayashi, N.; Kaji, M. *J. Chem. Soc., Dalton Trans.* **1984**, 793. (b) Yamase, T.; Watanabe, R. *J. Chem. Soc., Dalton Trans.* **1986**, 1669.

(11) (a) Papaconstantinou, E.; Dimotikali, D.; Politou, A. *Inorg. Chim. Acta* **1980**, *46*, 155. (b) Papaconstantinou, E.; Ioannidis, A. *Ibid.* **1983**, *75*, 235. (c) Dimotikali, D.; Papaconstantinou, E. *Ibid.* **1984**, *87*, 177. (d) Ioannidis, A.; Papaconstantinou, E. *Inorg. Chem.* **1985**, *24*, 439. (e) Argitis, P.; Papaconstantinou, E. *Ibid.* **1986**, *25*, 4386.

(12) Papaconstantinou, E. *J. Chem. Soc., Chem. Commun.* **1982**, 12.

(13) (a) Darwent, J. R. *J. Chem. Soc., Chem. Commun.* **1982**, 798. (b) Akid, R.; Darwent, J. R. *J. Chem. Soc., Dalton Trans.* **1985**, 395.

(14) Ward, M. D.; Brazdil, J. F.; Grasselli, R. K. *J. Phys. Chem.* **1984**, *88*, 4210.

(15) Savinov, E. N.; Saidkhanov, S. S.; Parmon, V. N.; Zamaraev, K. I. *Dokl. Phys. Chem. SSSR* **1983**, *272*, 741 and references cited therein.

(16) (a) Nomiya, K.; Sugie, Y.; Miyazaki, T.; Miwa, M. *Polyhedron* **1986**, *5*, 1267. (b) Nomiya, K.; Miyazaki, T.; Maeda, K.; Miwa, M. *Inorg. Chim. Acta* **1987**, *127*, 65.

(17) Hill, C. L.; Bouchard, D. A. *J. Am. Chem. Soc.* **1985**, *107*, 5148.

(18) (a) Renneke, R. F.; Hill, C. L. *J. Am. Chem. Soc.* **1986**, *108*, 3528. (b) Renneke, R. F.; Hill, C. L. *J. Am. Chem. Soc.*, preceding paper in this issue.

(19) Prosser-McCartha, C. M.; Kadkhodayan, M.; Williamson, M. M.; Bouchard, D. A.; Hill, C. L. *J. Chem. Soc., Chem. Commun.* **1986**, 1747.

(20) Williamson, M. M.; Bouchard, D. A.; Hill, C. L. *Inorg. Chem.* **1987**, *26*, 1436.

(21) Fox, M. A.; Cardona, R.; Gaillard, E. *J. Am. Chem. Soc.* **1987**, *109*, 6347.

(22) Colored solutions of heteropoly compounds in organic solvents have been noted before. See work cited in ref 1 and: Umland, F.; Wuensch, G. *Z. Anal. Chem.* **1967**, *225*, 362.

(23) A preliminary note on the picosecond spectroscopy of the $H_3PW_{12}O_{40}$/NMP system has appeared: Schmidt, J. A.; Hilinski, E. F.; Bouchard, D. A.; Hill, C. L. *Chem. Phys. Lett.* **1987**, *138*, 346.

(24) (a) Wu, H. *J. Biol. Chem.* **1920**, *43*, 189. (b) Rocchiccioli-Deltcheff, C.; Fournier, M. Franck, R.; Thouvenot, R. *Inorg. Chem.* **1983**, *22*, 207. The α isomer is specified here, for although the β isomer of $PW_{12}O_{40}{}^{3-}$ has yet to be well characterized, we have evidence that it exists and can be present as a minor impurity in the α isomer.

complexes, **1**–DP, were susceptible to reduction by metal spatulas, all polyoxometalate species in the studies reported here were manipulated with glass spatulas.

Methods. The procedures for the acquisition of ^{1}H, ^{31}P, ^{17}O, and ^{183}W NMR spectra were described previously.[17,20,25] The internal standards used for the ^{183}W, ^{17}O, and ^{31}P NMR spectra were 2.0 M aqueous (D_2O) Na_2WO_4, natural-abundance ^{17}O in H_2O, and 85% H_3PO_4, respectively. All chemical shifts reported employ negative chemical shifts to higher fields. The ^{31}P NMR spectra for the T_d α-$PW_{12}O_{40}^{3-}$ derivatives, although recorded for this work, were minimally informative for two reasons and thus are not addressed here. First, the buried phosphorus nucleus within any given isostructural series of phosphorus-containing heteropoly compounds is minimally responsive to changes in solvent.[26] Second, the small changes in the chemical shifts seen for a series of α-$PW_{12}O_{40}^{3-}$ derivatives including **1**–DP, DP = NMP, TMU, and DMEU, were attributable to differences in the bulk magnetic susceptibility of the solvent.[27] The infrared and electronic absorption spectra were recorded as described earlier.[17] Microanalyses were performed by Atlantic Microlabs, Atlanta, GA (carbon, hydrogen, nitrogen), and by Galbraith Laboratories, Knoxville, TN (phosphorus, tungsten).

Oxidative titrations of the reduced heteropolytungstates (heteropoly blues or HPBs) were made using standard solutions of dichromate or ceric ion. Permanganate-based oxidative titrations of the heteropoly blues were less satisfactory. Titrations were monitored by electronic absorption spectroscopy (disappearance of the blue chromophore of the heteropoly blue species).

***α*-Dodecatungstophosphoric Acid Hexakis(*N*-methylpyrrolidinone), $[(NMP)_2H]_3[PW_{12}O_{40}]$, 1–NMP.** To a solution of 5.0 g (1.67 mmol) of α-$H_3PW_{12}O_{40}\cdot nH_2O$, $n \simeq 6$, in 10 mL of water was added 1.0 mL (10.4 mmol) of *N*-methylpyrrolidinone. The resulting precipitate was collected on a fine frit, sucked as dry as possible, and crystallized several times in the dark from hot acetonitrile to yield 4.10 g of yellow solvate-free photosensitive crystals of **1**–NMP. ^{1}H NMR in 100% CD_3CN (for conditions of dissociation of **1**–NMP in solution, see Results and Discussion): 4.933 (s, br, ~3 H), 3.615 (t, J = 7.32 Hz, 12 H), 2.942 (s, 18 H), 2.655 (t, J = 7.98 Hz, 12 H) (q, 1.92, J = 7.42 Hz, 12 H). ^{1}H NMR in 100% DMSO-d_6: 3.303 (t, J = 7.14 Hz, 12 H), 2.692 (s, 18 H), 2.177 (t, J = 8.18 Hz, 12 H), 1.916 (q, J = 7.98 Hz, 12 H). ^{17}O NMR[25] in 100% NMP: 773.5 (s, terminal W=O), 447.0 and 417.8 (2 s, corner and edge-sharing W—O—W).[25b] ^{17}O NMR for α-$H_3PW_{12}O_{40}$ in 100% CD_3CN: 776.2 (s, terminal W=O), 437.2 and 409.5 (2s, corner and edge-sharing W—O—W)]. ^{183}W NMR in 100% NMP: −83.51 and −83.64 (d, all W). IR (cm^{-1}): 2990 (sh), 2942 (w), 2900 (w), 1670 (sh), 1662 (m), 1560 (m), 1536 (m), 1489 (w), 1460 (m), 1430 (m), 1360 (w), 1267 (m), 1195 (sh), 1119 (m), 1082 (vs), 982 (vs), 950 (s), 900 (vs), 810 (vs,br), 615 (s), 520 (s), 462 (w), 391 (s), 343 (w), 270 (w). Anal. Calcd for $C_{30}H_{63}N_6O_{46}PW_{12}$ (solvate free **1**–NMP): C, 10.37; H, 1.65; N, 2.42; P, 0.89; W, 63.49. Found: C, 10.41; H, 1.61; N, 2.40; P, 0.85; W, 63.50.

***α*-Dodecatungstophosphoric Acid Hexakis(1,1,3,3-tetramethylurea), $[(TMU)_2H]_3[PW_{12}O_{40}]$, 1-TMU.** To a 60-mL Gooch crucible was added 20 g (6.7 mmol) of α-$H_3PW_{12}O_{40}\cdot nH_2O$, $n \sim 6$, in 20 mL of water. The sample was vigorously stirred while 4.0 g (34 mmol) of tetramethylurea was added dropwise. The resulting yellow precipitate is collected, dried as much as possible by vacuum filtration, and then recrystallized twice from 80 °C acetonitrile in the dark to afford 16.70 g of photosensitive solvate-free yellow blocks of **1**–TMU. ^{1}H NMR in 100% CD_3CN (for conditions of dissociation of **1**–TMU in solution, see Results and Discussion): 5.26 (s, br, 3 H), 2.93 (s, 24 H). ^{1}H NMR in 100% DMSO-d_6: 2.686 (s). ^{17}O NMR[25] in 100% TMU: 775.0 (s, terminal W=O; only the downfield of the two types of doubly bridging oxygen was visible due to viscosity-induced broadening effects), 457.0 (s).[25b] ^{183}W NMR in 100% TMU: −85.06 and −85.19 (d, all W). IR (cm^{-1}): 2940 (m), 2806 (w), 1770 (m), 1645 (sh), 1590 (s), 1565 (s), 1555 (s), 1472 (m), 1454 (s), 1400 (s), 1248 (m), 1167 (s), 1078 (vs), 983 (vs), 891 (vs), 810 (vs, br), 790 (m), 609 (m), 520 (s), 389 (vs), 343 (vs), 268 (m). Anal. Calcd for $C_{30}H_{75}N_{12}O_{46}PW_{12}$: C, 10.07; H, 2.11; N, 4.70; P, 0.87; W, 61.67. Found: C, 10.11; H, 2.12; N, 4.67; P, 0.87; W, 61.35.

***α*-Dodecatungstophosphoric Acid Hexakis(1,3-dimethyl-2-imidazolidinone), $[(DMEU)_2H]_3[PW_{12}O_{40}]$, 1–DMEU.** To a 50-mL Erlenmeyer flask was added 5.0 g (1.67 mmol) of α-$H_3PW_{12}O_{40}\cdot nH_2O$, $n \sim 6$, in 10 mL of H_2O. To the homogeneous solution was added dropwise with stirring 1.1 mL (9.23 mmol) of 1,3-dimethyl-2-imidazolidinone. The resulting orange precipitate was recrystallized three times from acetonitrile at 80 °C in the dark to afford 4.2 g of orange very photosensitive crystals of **1**–DMEU. ^{1}H NMR in 100% CD_3CN: 6.02 (s, br, 3 H), 3.53 (s, 24 H), 2.87 (s, 36 H). ^{1}H NMR in 100% DMSO-d_6: 3.197 (s, 24 H), 2.625 (s, 36 H), 4907 (s, br, 3 H). ^{17}O NMR[25] in 100% DMEU: 764.9 (s, terminal W=O; only the downfield of the two types of doubly bridging oxygen was visible due to viscosity-induced broadening effects), 459.9 (s).[25b] ^{183}W NMR in 100% DMEU: −83.26 and −83.39 (s, all W). IR (cm^{-1}): 2940 (m), 2885 (m), 1640 (sh), 1612 (s), 1550 (s), 1454 (m), 1413 (s), 1390 (m), 1297 (s), 1250 (s), 1209 (m), 1079 (vs), 980 (vs), 895 (vs), 810 (vs, br), 755 (s), 650 (m), 605 (w), 574 (w), 522 (s), 390 (vs), 349 (s), 268 (m). Anal. Calcd for $C_{30}H_{63}N_{12}O_{46}PW_{12}$: C, 10.11; H, 1.78; N, 4.71; P, 0.87; W, 61.88. Found: C, 10.25; H, 1.82; N, 4.67; P, 0.87; W, 61.65.

X-ray Crystallography. A bright yellow crystal of **1**–TMU was obtained by slow evaporation of the acetonitrile/TMU solvent system open to atmospheric moisture at ambient laboratory temperature and in the dark. After mounting, the crystal was coated with epoxy cement. All crystallographic data were collected in complete darkness. Data collection and refinement parameters are summarized in Table SVI (supplementary material). The hardware and software for X-ray crystallographic determination were described previously.[20] The space group was uniquely determined to be the centric monoclinic $C2/c$ (No. 15). In accordance with the space group assignment, the phosphorus atom had to correspond to a special position of a 2-fold axis. A combination of conventional Patterson and direct methods techniques provided the locations of the phosphorus and six tungsten atoms. Subsequent Fourier synthesis and least-squares refinement provided locations for the remaining non-hydrogen atoms. The hydrogens of the TMU methyl groups were placed in their calculated positions and were allowed to "ride" through the refinement (C–H = 0.96 Å; $U_{iso}(H) = 1.2U_{eq}(C)$]. All non-hydrogen atoms were allowed to refine anisotropically. The final electron density difference map was featureless with a maximum positive peak 1.33 e Å^{-3} at a distance of 1.01 Å from W2. The final residuals were R = 0.0387 and R_w = 0.0324 (Table SVI). The ratio of variables to reflections was 8.6. The data were corrected for absorption by semiempirical (ψ scan) methods.[28] An empirical isotropic extinction parameter,[29] e, was refined to a value of 0.000 01 in the expression $F_{cor} = F_c/[1 + eF_c^2/\sin 2\theta]^{0.25}$. A weighting scheme utilizing the expression $w = [\sigma^2(F) + gF^2]^{-1}$ (where g = 0.000 05) was implemented. Neutral atom scattering factors were used.[30] The final positional and thermal parameters are given in Table SVII (supplementary material).

Assessment of Association Constants. Several spectrometric and graphical methods were used to evaluate the interactions between DP and the heteropolytungstate in the **1**–DP complexes in solution. Not surprisingly, neither Benesi–Hildebrand plots[31] nor Foster–Hammick–Wardley plots[32] were linear. Both types of plots are most suitable for 1:1 association complexes or for intermolecular complexes where only two populations of species are present at equilibrium. This is clearly not the case for **1**–DP in DP/CH_3CN systems. As a consequence, extracting quantitative information for such systems from either Benesi–Hildebrand or Hammick–Foster–Wardley treatments alone is not possible. Furthermore, none of the ^{31}P, ^{17}O, or ^{183}W NMR nor the UV–visible data for **1**–DP in solution are unambiguously characteristic of a particular association species. The qualitative information from such treatments, however, indicates that several association complexes with different ratios of DP to polyoxotungstate are present in solution and that this ratio varies with the mole fraction of DP in the medium, with complexes containing larger values of $[DP]/[\alpha\text{-}PW_{12}O_{40}^{3-}]$ predominating at high DP concentration.

Photochemical Apparatus and Measurements. The light sources used in this work were 1000-W Xe arc lamps (Oriel) equipped with temperature-controlled water-based infrared filters and various lenses to focus the light beam on the reaction apparatus. The cutoff and other filters were placed in all cases after the infrared filter and before the secondary focusing lens. Photochemical experiments were conducted in both 1-cm path length quartz cuvettes and 10-mm-i.d. NMR tubes adapted for anaerobic work. The quartz cuvettes were equipped with micro magnetic stirring bars, high-vacuum stopcocks, and standard-taper ground-glass

---

[25] (a) Sample preparation techniques for ^{17}O-enriched complexes: Filowitz, M.; Ho, R. K. C.; Klemperer, W. G.; Shum, W. *Inorg. Chem.* **1979**, *18*, 93. (b) The triply bridging internal oxygen atoms of the **1**–DP complexes were not visible by ^{17}O NMR since they are not enriched in ^{17}O.

[26] Massart, R.; Constant, R.; Fruchart, J. M.; Ciabrini, J. P.; Fournier, M. *Inorg. Chem.* **1977**, *16*, 2916.

[27] Lagodzinskaya, G. V.; Klimenko, I. Y. *J. Magn. Reson.* **1982**, *49*, 1.

[28] North, A. C. T.; Phillips, D. C. Mathews, F. C. *Acta Crystallogr., Sect. A: Cryst. Phys., Diffr. Theor. Gen. Crystallogr.* **1968**, *A24*, 351.

[29] Larsen, A. C. *Acta Crystallogr.* **1967**, *23*, 664.

[30] Cromer, D. T.; Waber, J. T. *International Tables of X-ray Crystallogrphy*; Kynoch: Birmingham, England, 1974; Vol. IV, Table 2.2B.

[31] (a) Benesi, H. A.; Hildebrand, J. H. *J. Am. Chem. Soc.* **1948**, *70*, 3978. (b) Bent, H. E.; French, C. L. *Ibid.* **1941**, *63*, 568. (c) Benesi, H. A.; Hildebrand, J. H. *Ibid.* **1949**, *71*, 2703.

[32] Foster R.; Hammick, D. L.; Wardley, A. A. *J. Chem. Soc.* **1953**, 3817.

joints used for interfacing with dual-manifold vacuum lines. These modified cuvettes facilitated irradiation of the polyoxometalate solutions coupled with the direct monitoring of the reduced heteropolytungstic acid products during the photolysis. The cuvette holder in the photochemical apparatus was equipped with both a water-circulating constant-temperature (26 ± 2 °C) control system and a magnetic stirring system. For all kinetics measurements other than those involving picosecond absorption spectroscopy, 0.5 mM solutions of **1**–DP in DP, DP = TMU and DMEU, were prepared with the crystalline analytically pure solvate-free complexes and not the starting hydrated forms of α-$H_3PW_{12}O_{40}$. These kinetics measurements (constant illumination) involved monitoring the absorbance, *A*, of the one-electron heteropoly blue complex, α-$H_3PW_{12}O_{40}^{4-}$, at the low-energy λ_{max} (e.g., 752 nm for **1**–TMU in 100% TMU) with time. The physical integrity of the α-$PW_{12}O_{40}^{n-}$ moiety before and after irradiation in representative experiments, assessed by ^{183}W and ^{31}P NMR, indicated that no detectable decomposition of the T_d Keggin structure had taken place as a result of the photochemical or subsequent dark processes.

The experimental procedures for using 10-mm-i.d. NMR tubes to follow the catalytic photochemical polyoxometalate-based reactions under anaerobic conditions were described earlier.[17]

Picosecond Spectroscopy. The picosecond laser system used for time-resolved absorption spectroscopy in these experiments is similar to that described previously.[23,33] The modified Quantel International YG-402 laser consists of an actively–passively mode-locked Nd:YAG oscillator and Nd:YAG amplifiers. Excitation pulses exhibiting a half-width of ~30 ps at 355 or 266 nm were generated from the 1064-nm fundamental by means of appropriate harmonic-generating crystals. The energies of the excitation pulses were measured by diverting ~10% of each pulse into the probe (Model RjP-735) of an energy meter (Model Rj-7200, Laser Precision Corp.) and were in the range 0.1–0.5 mJ/pulse. The beam diameter at the sample was ~2 mm.

The absorbance change induced upon excitation of the sample was monitored at a selected time after excitation by means of a 30-ps continuum pulse. This white-light probe pulse was generated when the sufficiently energetic portion of the split, original 1064-nm pulse was focused into a cell that contained a mixture of H_2O and D_2O. These probe pulses were directed through a sample cell and a reference cell and focused at the slit of a 0.32-m spectrograph (Model HR-320, Instruments SA). The output of the spectrograph was imaged onto an EG&G Princeton Applied Research Corp. (PAR) two-dimensional silicon intensified target detector (Model 1254E) coupled to an EG&G PAR Model 1216 multichannel detector controller. This detector controller was interfaced with an IBM personal computer that controlled necessary optical hardware and electronics during the course of data acquisition, processed the data, and presented the data graphically.

To improve the signal-to-noise ratio, each difference absorption spectrum is the result of at least 300 excitation laser shots. The spectra illustrated in Figures 5 and 6 were smoothed according to the method described by Savitsky and Golay[34] in which a ~9-point (1 nm/point) smoothing window was employed. A difference absorption spectrum spanning a wavelength range from 400 to 750 nm is the result of two overlapping spectra recorded in the 400–640-nm and the 555–750-nm regions at a selected time postexcitation. To acquire data for each transient absorption spectrum, the sample was flowed through a 2- or 5-mm path length fused silica flow cell at a rate sufficient to replace the volume that was exposed to the excitation pulses impinging upon the sample at a rate of 10 pulses/s. Sample solutions were replaced when needed to ensure that the data were not affected by irreversible photochemical changes in the sample.

Results and Discussion

General Spectroscopic and Photochemical Behavior of Heteropolytungstates in Dipolar Organic Media. The hydrated heteropoly acid α-$H_3PW_{12}O_{40}$ is a highly effective homogeneous catalyst for the catalytic photochemical oxidation (eq 6) and dehydrogenation (eq 7) of many dipolar aprotic organic substrates, including the ones examined in this study, *N*-methylpyrrolidinone, 1,1,3,3-tetramethylurea, and 1,3-dimethyl-2-imidazolidinone. Although hundreds and perhaps far higher numbers of turnovers can be achieved with these systems, this paper focuses on stoichiometric or low-turnover conditions for these are most useful in addressing several of the energetic, structural, and photochemical features of this chemistry. Although no attempt has been made to ascertain the stability of these catalytic systems under high-turnover conditions, the heteropolytungstate catalysts showed by ^{31}P, ^{17}O, and ^{183}W NMR no evidence of degradation after several turnovers. The catalytic reactions proceed by the general processes illustrated above in eq 1–5, with the photochemical processes generating the oxidized substrates and the reduced polyoxometalate (eq 1–3) being more rapid than either reoxidation process (eq 4 and 5) regardless of whether or not the hydrogen-evolution catalyst Pt(0) was present. The consequent buildup of the chromophore of the reduced heteropolytungstate permits measurement of the initial rates associated with these systems. Unlike previous reports on systems for the catalytic photochemical oxidation or dehydrogenation of alcohols in aqueous solutions by heteropoly compounds,[12,13] added acid is not needed in the **1**–DP systems investigated here, either to maintain the physical integrity of the heteropoly anion or to facilitate production of adequate redox potentials so that reoxidation of the reduced polytungstates is favorable.

The effect of the organic medium on the charge-transfer absorption manifold and photoinduced redox chemistry of the heteropoly anion α-$PW_{12}O_{40}^{3-}$ qualitatively defines four types of behavior. The first type of behavior is characterized by little change in the electronic absorption spectrum relative to water and no discernable photochemistry under continuous-wave illumination with UV–visible light sources. This behavior, for example, is seen in acetonitrile, the most common solvent used for physical and chemical investigations of polyoxometalates after water. The second type of behavior is characterized by little change in the electronic absorption spectrum but demonstrable activity with respect to oxidation of the organic media and reduction of the heteropoly anion upon irradiation with UV–visible light sources. This behavior is exhibited by solutions of heteropoly compounds in alcohol, ethylene glycol, ether, or carboxylic acid solvents or in aqueous solutions of these organic materials. These media have in fact been the focus of all the studies of polyoxometalate photochemistry apart from our work.[9–16,21] The third type of behavior is characterized by substantial red shifts in the electronic absorption spectra of the heteropoly anion but little or no photoinduced redox chemistry upon irradiation. There were reports in the literature prior to our work of normally colorless heteropoly compounds forming colored solutions when dissolved in some organic media.[1,22] The composition of these solutions has not been quantitatively defined, and none were reported to display any photochemistry; thus, these systems fall into the third category. Perhaps the most marked case in point of this third type of behavior involves the dissolution of α-$PW_{12}O_{40}\cdot nH_2O$ in DMSO. These very yellow DMSO solutions absorb light hundreds of nanometers further into the visible than aqueous or acetonitrile solutions of these heteropoly acids, and yet they display little or no photochemistry. The fourth qualitative category involves α-$PW_{12}O_{40}^{3-}$ in several other dipolar organic media including amides, phosphoramides, and ureas. The α-$PW_{12}O_{40}^{3-}$ chromophore is red shifted, in some cases by hundreds of nanometers, and the solutions are very sensitive to photoredox chemistry. Irradiation anywhere in the lower energy region of the UV–visible chromophore of these systems results in reduction of α-$PW_{12}O_{40}^{3-}$ coupled with oxidation of the organic substrate.

Dissolution of α-$H_3PW_{12}O_{40}$ in NMP, the common amide solvent, produces a yellow solution, while dissolution of the complex in the urea solvents TMU and DMEU produces dark yellow and orange solutions, respectively. Crystals of the same color and photosensitivity of formula $[(DP)_2H]_3[\alpha\text{-}PW_{12}O_{40}]$ (**1**–DP), DP = NMP, TMU, or DMEU, can be isolated from these solutions. The best synthetic routes, described in the Experimental Section, produce analytically pure anhydrous and solvate-free complexes, **1**–DP. The spectra of **1**–DP complexes in DP solvent are effectively identical with those obtained from dissolving the hydrated α-$H_3PW_{12}O_{40}$ in the same DP. Although the similarity of the physical and photochemical properties of the **1**–DP complexes in the crystalline state and in solution (100% DP) suggests that the solid-state structures, $[(DP)_2H]_3[\alpha\text{-}PW_{12}O_{40}]$, approximate the solution structures of the complexes, the actual solution structures are unknown. At the present time there are no direct spectroscopic

---

(33) Hilinski, E. F.; Rentzepis, P. M. *Anal. Chem.* **1983**, *55*, 1121A.

(34) Savitzky, A.; Golay, M. J. E. *Anal. Chem.* **1964**, *36*, 1627.

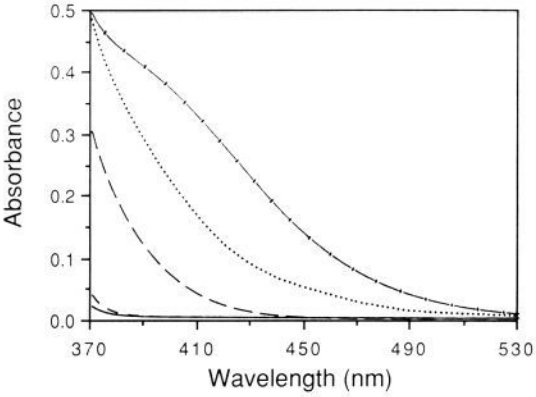

Figure 1. Electronic absorption spectra in the near-UV and blue regions for α-$H_3PW_{12}O_{40}$ in water and ethanol and **1**–DP in 100% DP, DP = NMP, TMU, and DMEU. All spectra were taken as 0.65 mM solutions at 25 °C with a 1.0-cm cell. Key: H_2O (—), EtOH (- - -), NMP (– –), TMU (···), DMEU (–·–).

methods capable of unambiguously identifying and quantifying the various possible photochemically active DP–polyoxotungstate association species in solution. For convenience only, the solution species will be designated henceforth as $[(DP)_2H]_3[\alpha\text{-}PW_{12}O_{40}]$.

Figure 1 compares the electronic absorption spectra of α-$PW_{12}O_{40}\cdot nH_2O$ in ethanol and H_2O with the spectra of **1**–DP in DP. The spectrum of α-$PW_{12}O_{40}\cdot nH_2O$ in H_2O is similar but slightly less red shifted than that in ethanol. Whereas solutions of α-$PW_{12}O_{40}\cdot nH_2O$ in alcohols produce negligible catalytic photochemical oxidation (eq 6) of the solvent when handled under fluorescent laboratory lights, solutions of **1**–DP in DP do exhibit such photochemistry. Not surprisingly from the visible spectrum, **1**–DMEU in DMEU (and crystalline **1**–DMEU) is sufficiently photosensitive that photoinduced redox chemistry in these systems cannot be avoided unless they are handled in a darkened laboratory. The relative overlap of the electronic absorption spectra of α-$PW_{12}O_{40}\cdot nH_2O$ in H_2O and in ethanol, as well as the complexes **1**–DP, in DP with the terrestrial solar spectrum from 350 to 600 nm are (relative to α-$PW_{12}O_{40}\cdot nH_2O$ in H_2O, 1.00) as follows: α-$H_3PW_{12}O_{40}$ in EtOH, 1.77; **1**–NMP in NMP, 7.57; **1**–TMU in TMU, 15.15; **1**–DMEU in DMEU, 21.59. The areas under the absorption curves in the visible region ($\lambda > 400$ nm) relative to **1**–NMP in NMP (1.00) are as follows: α-$PW_{12}O_{40}\cdot nH_2O$ in H_2O or EtOH, 0; **1**–TMU in TMU, 6.49; **1**–DMEU in DMEU, 14.70.

X-ray Crystallographic Characterization of 1–TMU. For the steady-state and time-resolved photochemical and photophysical studies of **1**–DP dissolved in DP and crystalline **1**–DP to be optimally informative, we needed to undertake several physical studies to assess a number of the structural and electronic features of these systems first. Diffraction-quality single crystals of all three **1**–DP complexes, DP = NMP, TMU and DMEU, were obtained; however, only **1**–TMU afforded crystals that were free of the inversion symmetry disorder that has plagued many attempted crystallographic structure determinations of heteropoly complexes with the Keggin structure $(\alpha\text{-}X^{n+}M_{12}O_{40})^{(8-n)-}$.[35,36] The TMU complex, $[(TMU)_2H]_3[\alpha\text{-}PW_{12}O_{40}]$, crystallized solvate free in the monoclinic space group $C2/c$, with a = 21.3221 (87) Å, b = 13.8654 (47) Å, c = 24.8262 (71) Å, β = 100.830 (28)°, V = 7208.87 (4.23) Å^3, and Z = 4, and refined smoothly to yield low values for the final residuals (Experimental Section; Table SVI). A combination ORTEP and atom-numbering diagram for **1**–TMU is shown in Figure 2, and selected bond distances and angles for this complex are given in Tables SVIII and SIX, respectively (supplementary material). The six TMU moieties per α-$PW_{12}O_{40}{}^{3-}$ are clearly present as three hydrogen-bonded dimers with the O–O distances indicated on Figure 2 by thin double lines. The hydrogen bonding is through the TMU oxygens in all cases, as expected on the basis of the ground-state electronic structure and basicity of amides and ureas and on numerous structural investigations of amide–metal or amide–proton interactions in both biological[37] and nonbiological systems.[38] The lengths of the hydrogen bonds, O(a)–O(a′), O(b)–O(b′), and O(c)–O(c′) of 2.45, 2.47, and 2.33 Å, respectively, indicate fairly strong hydrogen bonds. In one case, that of $[(TMU)_2H]^+$ dimer b, the hydrogen atom was located. The thermal motion is quite large for some of the TMU non-hydrogen atoms, with those of TMUc being particularly large. The motion of these atoms, as indicated in Figure 2, is primarily perpendicular to the mean plane of the TMU unit.

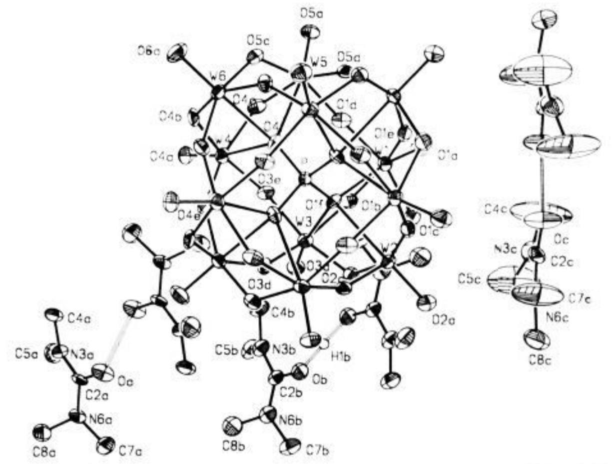

Figure 2. Combination ORTEP and atom-numbering diagram of **1**–TMU. Long hollow lines between the urea oxygens, O(a)–O(a′), O(b)–O(b′), and O(c)–O(c′), indicate the TMU–TMU hydrogen bonds. The TMU hydrogen atoms have been omitted for clarity. Thermal ellipsoids are at the 30% probability level.

Table I. Short Solvate–Polyoxometalate Nonbonding Distances in **1**–TMU

solvate molecule	nearest nonbonded solvate non-H atom	α-$PW_{12}O_{40}{}^{3-}$ O involved in bonding	dist, Å
	Shortest Contact for Each Solvate Molecule		
TMU(a)	C(a)	O(5a)	2.896 (shortest)
TMU(c)	N(oc)	O(2a)	3.267
TMU(b)	C(7b)	O(3a)	3.307
	Other Short Contacts		
TMU(a)	N(3a)	O(5a)	3.236
TMU(b)	N(6b)	O(3a)	3.324

A number of common photochemically inactive heteropoly acids have been characterized crystallographically.[39-41] Hydrated α-$H_3PW_{12}O_{40}$ itself was both the subject of the first structural determination of this class of compounds by Keggin[40] and the

---

[35] For a reasonable description of this symmetry problem see: Evans, H. T., Jr.; Pope, M. T. *Inorg. Chem.* **1984**, *23*, 501.

[36] Orange single crystals of the **1**–DMEU·$2H_2O$ crystallized in triclinic space group $P\bar{1}$ (No. 2) with a = 12.501 (5) Å, b = 12.554 (6) Å, c = 13.898 (9) Å, α = 93.79 (4)°, β = 114.83 (3)°, γ = 104.53 (3)°, V = 1879 (2) Å^3, Z = 1. The structure had the noncentric $PW_{12}O_{40}{}^{3-}$ molecules at inversion centers in the unit cell, a disorder problem encountered in several other X-ray crystallographic structure determinations of T_d Keggin heteropoly compounds in other laboratories,[35] and in our laboratory. Although the complex refined to a final R = 0.10, the disorder prohibits an analysis of the detailed structural features of this complex. It should be noted here that polyoxometalates with totally incorrect polyoxometalate skeletons have refined to R values of 14%. A key case in point: Besecker, C. J.; Day, V. W.; Klemperer, W. G.; Thompson, M. R. *J. Am. Chem. Soc.* **1984**, *106*, 4125.

[37] Sigel, H.; Martin, R. B. *Chem. Rev.* **1982**, *82*, 385.

[38] (a) Hill, C. L.; Williamson, M. M. *Inorg. Chem.* **1985**, *24*, 2836. (b) Rao, Ch. P.; Rao, A. M.; Rao, C. N. R. *Inorg. Chem.* **1984**, *23*, 2080 and references cited in each.

[39] Review of early polyoxometalate structural investigations: Evans, H. T. *Perspect. Struct. Chem.* **1971**, *4*, 1.

[40] Keggin, J. F. *Proc. R. Soc. London, Ser. A* **1934**, *A144*, 75.

[41] Brown, G. M.; Noe-Spirlet, M.-R.; Busing, W. R.; Levy, H. A. *Acta Crystallogr., Sect. B: Struct. Crystallogr. Cryst. Chem.* **1977**, *B33*, 1038.

subject of what is probably the most precise polyoxometalate crystallographic structural determination in the literature, the neutron diffraction study of Brown et al.[41] The protons associated with the Keggin heteropolytungstic acids are usually bound to the solvate (water) molecules and not to the oxygens of the polyoxoanion.[42] The protonated water molecules in the structures of conventional heteropoly acids of tungsten, however, are usually found in networks rather than in discrete protonated dimers as in the case of **1**–TMU. It is of interest to note that the previously characterized heteropolymolybdate complex $[(DMA)_2H]_3PMo_{12}O_{40}$, a complex of high photosensitivity but one that did *not* display a chromophore greatly red shifted from the chromophore of $PMo_{12}O_{40}^{3-}$ in water or alcohol solvents, showed a complex network of close nonbonding interactions between the $[(DMA)_2H]^+$ and $PMo_{12}O_{40}^{3-}$ units in the unit cell.[20] Again, no such network of close nonbonding interactions exists in the unit cell of **1**–TMU (a packing diagram is available in supplementary material).[43] The shortest nonbonding interactions between the $[(TMU)_2H]^+$ and α-$PW_{12}O_{40}^{3-}$ units in **1**–TMU, summarized in Table I, are not likely to amount to more than 2 kcal/mol per interaction.

More importantly, it is apparent upon examination of all bonding and nonbonding distances that there are no covalent or hydrogen-bonding contacts between the $[(TMU)_2H]^+$ units and the heteropoly anion. Clearly the data available at present indicate that the source of the red shifts of the electronic absorption and photochemical action spectra of **1**–DP induced by the proximity of the $[(DP)_2H]^+$ units to the α-$PW_{12}O_{40}^{3-}$ unit arises from electronic features not transmitted through strong directed and localized bonds between these two units.

Photochemistry of the 1–DP Complexes. The dominant feature of the colored photosensitive **1**–DP complexes when dissolved in a solvent other than DP is a disruption of the $[(DP)_2H]_3[\alpha$-$PW_{12}O_{40}]$ structure, and with it, a loss of color and photosensitivity of the solution beyond 400 nm. This disruption of the **1**–DP complexes may be more complete in deuteriated acetonitrile than in deuteriated DMSO. ^1H NMR spectra of all three **1**–DP complexes at <1 mM in both CD_3CN and DMSO-d_6 show chemical shifts for DP similar to but not identical with those exhibited by pure DP in the same solvent. These minor differences appear to be consequence of the much higher ionic strength of the **1**–DP solutions relative to the DP solutions. The protons in the $[(DP)_2H]^+$ units become associated with the small exchangeable proton peak resulting from the trace of residual H_2O present in these solvents and are not readily seen in all cases. Examination of the ^{31}P, ^{183}W, and ^{17}O (23 atom % enriched in ^{17}O) NMR spectra of all three complexes **1**–DP in DP indicates that the T_d α-$PW_{12}O_{40}^{3-}$ unit is intact in solution in all three cases. No other phosphorus- or tungsten-containing material other than α-$PW_{12}O_{40}^{3-}$ is generated upon dissolution of **1**–DP in DP or in acetonitrile. The interactions between the $[(DP)_2H]^+$ units and the α-$PW_{12}O_{40}^{3-}$ units that give rise to the spectral shifts and the photochemical behavior are formed reversibly. Indeed the purification of the complexes **1**–DP by recrystallization from acetonitrile results in complete disruption followed by re-formation of the colored species.

The time dependence of the production of the reduced heteropolytungstate chromophore upon irradiation of **1**–DMEU in DMEU is illustrated in Figure 3. The absorption maxima of the reduced complex (494, 752 nm) and ratios of the molar extinction coefficients at these two maxima in the A_∞ spectrum were similar to those of the α-$PW_{12}O_{40}^{4-}$ chromophore obtained in our laboratory in acetonitrile and in the laboratory of Pope in water.[44]

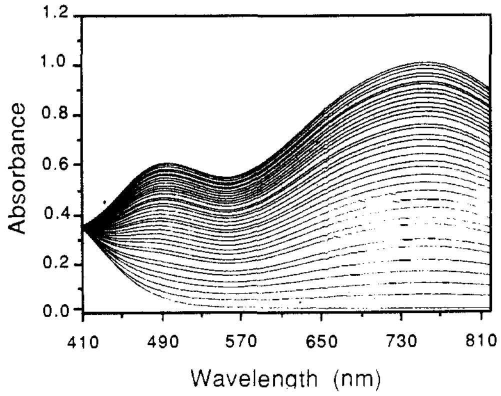

Figure 3. Time dependence of the production of the reduced α-$PW_{12}O_{40}^{4-}$ chromophore upon irradiation of 0.45 mM solution of **1**–DMEU in 100% DMEU at 1-min intervals. Conditions: cell path length, 1.0 cm; irradiation time, 35 m; λ, >395 nm light (A_∞ reached in 1 h).

Oxidative titration of the final heteropoly blue compound, most satisfactorily achieved with ceric or dichromate titrants and not permanganate, indicated approximately 1.1 and 1.3 electron/α-$PW_{12}O_{40}^{n-}$ moiety at A_∞ for **1**–DP in DP, DP = TMU and DMEU, respectively. Control experiments indicated that the rate of reoxidation of the α-$PW_{12}O_{40}^{4-}$ (eq 5) under the reaction conditions (no Pt(0) or other hydrogen-evolution catalyst present) was approximately 2 orders of magnitude slower than the initial rate of α-$PW_{12}O_{40}^{4-}$ formation for **1**–DP in DP systems, DP = TMU or DMEU. Figure 3 illustrates two interesting points pertinent to the kinetics of these photochemical processes. There are no changes in the absorption maxima of the heteropolytungstate photoreduction product throughout the course of the photoreduction. In most, but not all, cases in the literature illustrating the time dependence of the UV–visible spectra resulting from photoreduction of polyoxometalates by organic substrates, the λ_{max} as well as the overall shape of the absorption envelope show substantial changes as a function of irradiation time. In many of these cases, this results from the fact that several heteropoly blue species in different states of reduction are formed as a function of time under steady-state illumination.[10,11] However, in Figure 3 an isosbestic point at ca. 412 nm is exhibited. Both the constancy of the chromophore of the reduced heteropolytungstate in the **1**–DMEU/DMEU system and the isosbestic point are in accord with the existence of the one-electron heteropoly blue product, α-$PW_{12}O_{40}^{4-}$, as the only reduced chromophore at A_∞. The temporal behavior of the photoredox processes for **1**–TMU in TMU and **1**–DMEU in DMEU are very similar. The temporal behavior for **1**–NMP in NMP is rendered more complex because of slightly faster reoxidation rates (eq 5) for α-$PW_{12}O_{40}^{4-}$ in this system.

The initial rates of α-$PW_{12}O_{40}^{4-}$ production for **1**–TMU in TMU using the cutoff filters λ > 375 nm, λ > 395 nm, λ > 420 nm, λ > 435 nm, and λ > 455 are, respectively, 6.4 × 10^{-2}, 2.7 × 10^{-2}, 5.7 × 10^{-3}, 2.3 × 10^{-3}, and ~0 M m^{-1}. The analogous initial rates for **1**–DMEU in DMEU using the cutoff filters λ > 375 nm, λ > 395 nm, λ > 420 nm, λ > 455 nm, λ > 475 nm, λ > 495 nm, and λ > 515 nm are, respectively, 8.3 × 10^{-2}, 4.0 × 10^{-2}, 2.1 × 10^{-2}, 4.2 × 10^{-3}, 2.8 × 10^{-3}, 9.2 × 10^{-4}, and ~0 M m^{-1}. Although the picosecond spectroscopic behavior discussed below clearly establishes that redox events are taking place between the DP substrate and α-$PW_{12}O_{40}^{3-}$ on a time scale faster than diffusion, the kinetics data summarized above and in Figure 4 involve monitoring the production of α-$PW_{12}O_{40}^{4-}$ under conditions of steady-state illumination. The output of the light source is relatively constant throughout the near-UV and visible regions. As exemplified in Figure 4 by the **1**–TMU system, these systems display a degree of photoinduced redox chemistry that is proportional to the incident light on the system from 375 to 455 (and

---

(42) For an exemplary study describing protonation on polyoxometalate oxygen atoms, see a recent definitive report of protonation sites in $H_3V_{10}O_{28}^{3-}$: Day, V. W.; Klemperer, W. G.; Maltbie, D. J. *J. Am. Chem. Soc.* **1987**, *109*, 2991.

(43) Interestingly, the angles between the mean DMA planes in the three $[(DMA)_2H]^+$ groups of $[(DMA)_2H]_3PMo_{12}O_{40}$ are seemingly randomly oriented (64.1, 68.5, 95.9°), while the angles between the mean TMU planes in the three $[(TMU)_2H]^+$ groups of **1**–TMU are nearly coplanar (0.1 0.1, 12.2°).

(44) Varga, G. M., Jr.; Papaconstantinou, E.; Pope, M. T. *Inorg. Chem.* **1970**, *9*, 662.

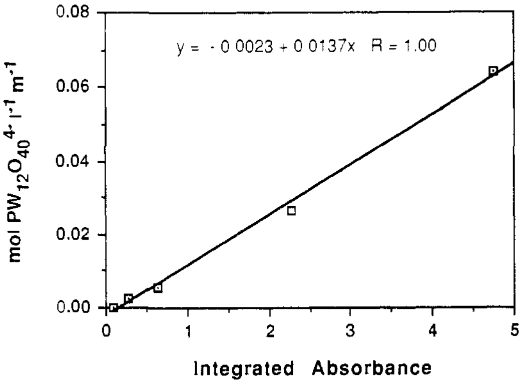

Figure 4. Initial reaction rates for production of the blue chromophore of the α-$PW_{12}O_{40}^{4-}$ reduction product from 1–TMU in 100% TMU plotted as a function of the integrated areas under the absorption curves for several different spectral regions, defined by the cutoff filters used ($\lambda > 375$ nm, $\lambda > 395$ nm, $\lambda > 420$ nm, $\lambda > 435$ nm, $\lambda > 455$). Equation of the best fit line (drawn) and correlation coefficient are given at the top.

greater) nm. Indeed, the quantum yields for production of the reduced heteropolytungstate are relatively constant throughout the low-energy region in all three systems where the chromophores absorb light. The quantum yields of **1**–TMU in TMU and **1**–DMEU in DMEU at 320 nm are 0.27 and 0.17, respectively. These results suggest that the systematic maximization of these red shifts could lead to polyoxometalate-based catalytic photochemical redox processes that would proceed at reasonably high turnover rates utilizing only sunlight as the light source.

Nature of the Charge-Transfer Excited States Associated with the Photochemistry of 1–DP Systems. The spectroscopic and photochemical properties of the systems constituted by **1**–DP in DP solvent can be attributed to two molecular phenomena. These phenomena, intermolecular charge-transfer (CT) behavior[45,46] and solvent-perturbed intramolecular charge-transfer behavior, are in principle distinct. The **1**–DP systems display the properties of classical intermolecular CT complexes, also described as electron donor–acceptor (EDA) complexes. Among other characteristics, dissolution of hydrated **1** in DP produces lower energy electronic absorption bands that are not present in either **1** or DP alone. DMEU, which is more easily oxidized than NMP, causes a greater increase in longer wavelength absorbances of solutions of **1** in DMEU than those observed for **1** in NMP. This behavior is expected for EDA complexes.[45,46] These lower energy bands may be attributed to intermolecular CT transitions. While CT bands of this type may exhibit pronounced maxima for a variety of EDA complexes, such as those formed between organic molecules, many examples exist for which the maxima of the CT bands are not well resolved from the intracomponent absorption bands. An example of the latter situation, similar to the **1**–DP sytems, is the recently investigated anthracene–tetranitromethane EDA complex.[47] Examination of the absorption spectra of **1**–TMU and **1**–DMEU in Figure 1 reveals the presence of slight shoulders in the 400–420-nm region.

In general, excitation of an organic EDA complex within the CT absorption band results in electron transfer from the donor component to the acceptor component. The quantum yields for these photoredox processes[45–47] are quite often in the 0.1–0.3 range that is observed for **1**–DP in DP. For these reasons, the **1**–DP systems can be viewed as EDA complexes, with the organic molecules acting as the donor and the d^0 heteropolytungstate anion acting as the acceptor. The **1**–DP complexes should be placed in context with the large number of well-documented EDA complexes formed between two organic molecules[45–48] or between one or more organometallic moieties and an organic molecule.[49] As many of the classical organic EDA complexes are salts, such as the 1-alkylpyridinium halides,[48] held together by ionic forces and EDA interactions, so are those formed between **1** and DP.

Alternatively, the spectroscopic and photochemical characteristics of the **1**–DP systems at this time can reasonably be attributed to solvent perturbations of ligand-to-metal CT (LMCT) states involving donation of a nonbonding electron from oxygen to tungsten within a heteropolytungstate unit. The mechanism of photooxidation of alcohols and other substrates in the non-red-shifted polyoxometalate systems addressed in the literature has incorporated LMCT excited states as the species involved in the substrate activation processes.[9–14] LMCT excited states of α-$PW_{12}O_{40}^{3-}$ in **1**–DP could be quenched by electron transfer from an oxidizable organic substrate such as DP. Although not explicitly described for **1**, considerations[10b,50] of the electronic spectra of polyoxometalates have led to the assignment of absorptions for wavelengths longer than ~310 nm to promotion of a nonbonding electron from a tungsten-bridging oxygen to a tungsten. This type of transition is expected to be sensitive to perturbations by solvent and other interacting molecules.

The concepts of a classical intermolecular CT transition and a perturbed LMCT transition are descriptions of the extremes of possible phenomena associated with **1**–DP interactions. Our working description of **1**–DP as an EDA complex is made with the understanding that, in the classical sense, it is not a complete description for **1**–DP and a perturbation of the LMCT transition must also be considered for these systems. A more detailed understanding of the relative contributions of these two phenomena to the photochemical behavior of **1**–DP awaits the results of further experiments.

Picosecond Spectroscopy of 1–NMP and 1–DMEU. With the physical and photochemical characteristics of the **1**–DP systems delineated to a reasonable degree, we now turn to an examination of the light-induced phenomena associated with these systems in the picosecond time regime. The time-resolved spectroscopic studies of the bathochromically unaffected polyoxometalate–alcohol systems reported by the groups of Papaconstantinou,[12] Yamase,[10] and Darwent[13] indicated that the key photoredox processes were completed in less than the microsecond time resolution of their experiments. Our earlier report of the results of 355-nm excitation of **1**–NMP in NMP[23] revealed that the pertinent time scale for the photoredox phenomena associated with this system is picoseconds. In that report,[23] evidence was presented for at least two spectroscopically distinct forms of the polyoxometalate ion in the submicrosecond time regime. When 4.5 mM **1**–NMP in NMP was excited at 266 nm with a 30-ps laser pulse, the evolution of the electronic absorption spectrum between 400 and 750 nm proceeded in a manner that is the same within experimental error as that observed for the 355-nm excitation[23] of this system. Several possibilities exist for the event exhibiting a time constant of ~20 ps. These include (1) reorganization of NMP molecules in the solvation sphere surrounding the reduced polyoxometalate, (2) loss of NMP or $NMP^{\bullet+}$ from the Franck–Condon excited state of **1**–NMP, or (3) a shift of a proton after population of the Franck–Condon excited state of **1**–NMP. These possibilities represent modes of relaxation of the first-formed excited state $\{[(NMP)_2H^+]_3(\alpha\text{-}PW_{12}O_{40}^{3-})\}^*$ to a species exhibiting the absorption spectrum of α-$PW_{12}O_{40}^{4-}$ observed previously on a much longer time scale.[10b,12,13b]

To our knowledge, the absorption spectrum of $NMP^{\bullet+}$ has not been reported previously. In an effort to learn the wavelengths

---

(45) Mulliken, R. S.; Person, W. B. *Molecular Complexes*; Wiley-Interscience: New York, 1969; many references cited therein.

(46) Reviews of organic electron donor–acceptor complexes: (a) Foster, R. *Organic Charge-Transfer Complexes*; Academic: New York, 1969. (b) *Molecular Complexes*; Foster, R., Ed.; Crane, Russak and Co.; New York; 1973, Vol. 1; 1974, Vol. 2. (c) *Molecular Association*; Foster, R., Ed.; Academic: New York: 1975, Vol. 1; 1979, Vol. 2. (d) Kosower, E. *Prog. Phys. Org. Chem.* **1965**, *3*, 81. (e) Kosower, E. *Physical Organic Chemistry*; Wiley: New York, 1968; pp 179–195.

(47) (a) Masnovi, J. M.; Huffman, J. C.; Kochi, J. K.; Hilinski, E. F.; Rentzepis, P. M. *Chem. Phys. Lett.* **1984**, *106*, 20. (b) Masnovi, J. M.; Kochi, J. K.; Hilinski, E. F.; Rentzepis, P. M. *J. Am. Chem. Soc.* **1986**, *108*, 1126.

(48) Kosower, E. *J. Am. Chem. Soc.* **1958**, *80*, 3253.

(49) Kochi, J. K. *Organometallic Mechanisms and Catalysis*; Academic: New York, 1978; Part 3, and references cited therein.

(50) Taketa, H.; Katsuki, S.; Eguchi, K.; Seiyama, T.; Yamazoe, N. *J. Phys. Chem.* **1986**, *90*, 2959.

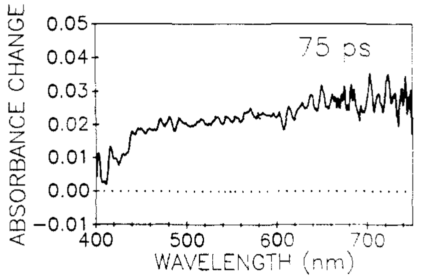

Figure 5. Difference absorption spectrum recorded 75 ps after 355-nm excitation of a 18 mM solution of α-$H_3PW_{12}O_{40}$ in CH_3CN. The average energy per laser pulse was 0.30 mJ; cell path length 2 mm.

over which NMP$^{\bullet+}$ absorbs and the contributions that this makes to the transient absorption spectra recorded for **1**–NMP in NMP, we excited the NMP–tetracyanoethylene (TCNE) EDA complex at 355 nm, a wavelength within the CT absorption band that exhibits maxima at 399 and 418 nm. Neither TCNE nor NMP individually absorbs at 355 nm. Picosecond-pulsed excitation within the CT bands of such complexes has been shown to lead to the generation of the cation radical–anion radical pair within the time duration of the laser pulse.[47,51] Excitation of a 15 mM solution of TCNE in NMP at 355 nm generated an absorption band that tails into the region near 450 nm and is the result of an electronic transition within TCNE$^{\bullet-}$. Although we previously reported that, within our limits of detection, the NMP$^{\bullet+}$ did not absorb light in the 420–750-nm region,[23] inspection of the spectra reveals that a very weak absorption band may exist near 640 nm that may be due to NMP$^{\bullet+}$. The weakness of this band is consistent with the spectrum assigned to DMEU$^{\bullet+}$ discussed below. The time-dependent behavior of these absorption bands observed for NMP–TCNE is consistent with that observed previously for EDA complexes of this type.[51] We cannot exclude the possibility that a portion of the absorption band exhibited by the excited NMP–TCNE EDA complex near 450 nm is not the result of an electronic transition within NMP$^{\bullet+}$. However, if the absorptions described above are due to NMP$^{\bullet+}$ they will have little effect on the appearance of the absorption spectra recorded at times after 355- or 266-nm excitation of **1**–NMP.

In the absence of materials that reduce the photochemically activated polyoxometalate, time-dependent absorbance changes evolve on a faster time scale. Excitation of 18 mM α-$H_3PW_{12}O_{40}{\cdot}nH_2O$ in CH_3CN at 355 nm gives rise to a series of transient absorption spectra. A broad weak absorption band (Figure 5) extending from 420 to 760 nm appears within the excitation pulse and decays to base line within 300 ps after excitation. This band can be assigned to an oxygen-to-tungsten LMCT state. On the basis of previous discussions of the electronic spectroscopy of polyoxometalates, this absorption band is similar to that of the heteropoly blue species, α-$PW_{12}O_{40}^{4-}$, whose color is due to intervalence CT transitions between tungsten(V) and tungsten(VI) and tungsten d–d transitions that give rise to absorption bands near 750 and 600 nm, respectively.[52] The electronic transition from the LMCT excited state to a higher energy excited state may be considered to involve similar types of excitations. If this LMCT excited state is responsible for the photoredox events reported with other substrates, any oxidizable substrate that is not within the sphere of influence of the polyoxometalate when it absorbs light must encounter the excited-state species prior to its decay in order to allow the redox process to occur.

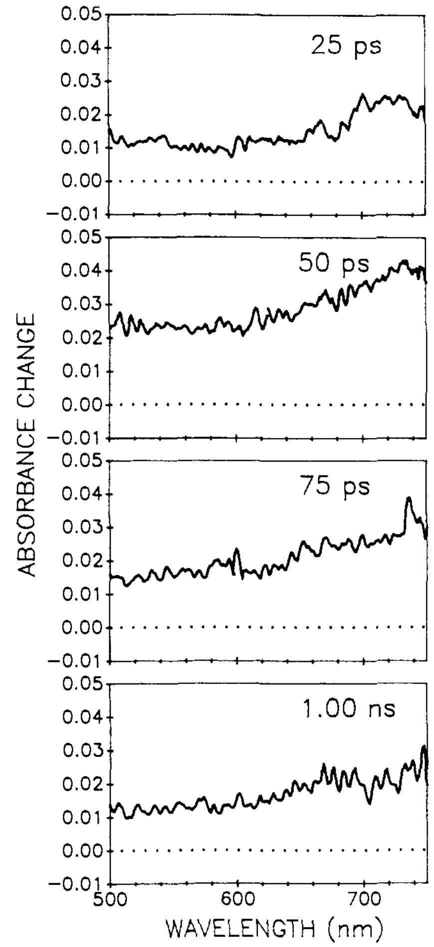

Figure 6. Difference absorption spectra recorded at selected times after 355-nm excitation of 4.5 mM **1**–DMEU in DMEU. The average energy per laser pulse was 0.32 mJ; cell path length 5 mm.

Excitation of **1**–DMEU in DMEU, another system exhibiting a tailing absorption into the visible region of the spectrum, results in transient phenomena illustrated in Figure 6. The series of the difference absorption spectra following 355-nm excitation of 4.5 mM **1**–DMEU in DMEU is different from that observed for **1**–NMP in NMP excited at either 355 or 266 nm. For the **1**–DMEU system, a prompt, pronounced increase in the 650–750-nm region occurs within the excitation laser pulse. After 50 ps, the intensity of the absorbance change decreases to values that are constant beyond 1 ns for the range of wavelengths from 400 to 750 nm. Upon excitation of the **1**–DMEU sample, an emission in the 400–530-nm region was detected in our spectral window of interrogation. For this series of spectra, emission from the sample was subtracted from the absorption data during the time of data acquisition.

To determine whether excitation of DMEU is responsible for any of the observed absorbance changes, transient absorption spectra were recorded after 355-nm excitation of DMEU alone. The ground-state absorbance of the neat DMEU sample contained in a 2-mm optical cell was 0.049 at 355 nm; this is compared to A_{355} = 1.4 for 4.5 mM **1**–DMEU in DMEU. The absorbance changes in the 400–750-nm region after subtraction of emission from DMEU* in the 400–500-nm region were less than 0.01 in the time regime from 0 to 100 ps after excitation.

While an attempt was made to determine whether DMEU$^{\bullet+}$ absorbs light in the 400–750-nm region in a manner analogous to that performed for NMP–TCNE EDA complex, it was found that this approach was inappropriate for the DMEU–TCNE EDA complex, which readily underwent a reaction via electron transfer as indicated by the presence of TCNE$^{\bullet-}$ in the steady-state electronic absorption spectrum of the solution. To obviate experimental problems associated with such a reactive DMEU–TCNE EDA complex, electron transfer from DMEU was at-

---

(51) (a) Hilinski, E. F.; Masnovi, J. M.; Amatore, C. Kochi, J. K.; Rentzepis, P. M. *J. Am. Chem. Soc.* **1983**, *105*, 6167. (b) Hilinski, E. F.; Masnovi, J. M.; Kochi, J. K.; Rentzepis, P. M. *J. Am. Chem. Soc.* **1984**, *106*, 8071.

(52) (a) Review on heteropoly blues: Pope, M. T. In *Mixed Valence Compounds*; Brown, D. B., Ed.; D. Reidel: Boston, 1980; pp 365–386. (b) Papaconstantinou, E.; Hoffman, M. Z. *Inorg. Chem.* **1982**, *21*, 2087. (c) Flynn, G. M.; Pope, M. T. *Inorg. Chem.* **1973**, *12*, 1626. (d) Fruchart, J. M.; Hervé, G.; Launay, J. P.; Massart, R. *J. Inorg. Nucl. Chem.* **1976**, *38*, 1627. (e) Papaconstantinou, E.; Pope, M. T. *Inorg. Chem.* **1970**, *9*, 667.

J. Am. Chem. Soc. **1988**, *110*, 5479–5489

tempted via encounter with the triplet excited state of chloranil (CHL), an approach used successfully in previous picosecond spectroscopic investigations to generate cation radicals of organic molecules.[53] When an acetonitrile solution containing 20 mM CHL and 70 mM DMEU was excited at 355 nm, the initial generation of ^{1}CHL* followed by its rapid conversion to ^{3}CHL* was observed in the expected manner.[53] The triplet–triplet absorption band of ^{3}CHL* at 510 nm decayed with concomitant appearance of the 450-nm band of CHL$^{\bullet+}$ and a new, weak absorption band in the 600–760-nm region, which increased from shorter to longer wavelengths. On the basis of previous behavior of electron donors in the presence of ^{3}CHL*, it appears likely that this weak 600–760-nm absorption band is a doublet doublet transition of DMEU$^{\bullet+}$.

With the detection of an absorption band attributable to DMEU$^{\bullet+}$, the prompt increase of the absorption in the 650–750-nm region resulting after 355-nm excitation of **1**–DMEU (Figure 6) could be due to the generation of DMEU$^{\bullet+}$ and α-$PW_{12}O_{40}^{4-}$. The decrease in the absorbance change occurring within 75 ps of excitation and remains constant for times longer than 1 ns after excitation may be the result of further reaction of DMEU$^{\bullet+}$ while α-$PW_{12}O_{40}^{4-}$ persists on this time scale. In the case of **1**–DMEU, it appears that both the oxidized donor and the reduced acceptor are detected within the excitation laser pulse, a behavior expected for an EDA complex.[47,51] The picosecond spectroscopic experiments reveal that photoredox chemistry of **1**–NMP and **1**–DMEU occurs on a subnanosecond time scale. Specific experiments to address other photophysical and photochemical features of these catalytic and radiant energy conversion systems are in progress.

Acknowledgment. C.L.H. thanks the National Science Foundation (Grant CHE-8715322) for support. E.F.H. and J.A.S. thank the National Science Foundation (Grant CHE-8605560) and the donors of the Petroleum Research Fund, administered by the American Chemical Society, for support. Grants from the National Science Foundation were used in part to purchase the 200- and 360-MHz spectrometers.

Registry No. **1**·6NMP, 110401-80-4; **1**·6TMU, 115140-67-5; **1**·6DMeU, 115140-68-6; α-$H_3PW_{12}O_{40}$, 1343-93-7.

Supplementary Material Available: Tables of anisotropic thermal parameters, calculated hydrogen positions, torsion angles, nonbonded distances, atomic coordinates, and bond lengths and angles, crystal data collection parameters, and a packing diagram of unit cell for $[(TMU)_2H]_3[\alpha\text{-}PW_{12}O_{40}]$ (**1**–TMU) (16 pages); listings of observed and calculated structure factors (24 pages). Ordering information is given on any current masthead page.

---

[53] Hilinski, E. F.; Milton, S. V.; Rentzepis, P. M. *J. Am. Chem. Soc.* **1983**, *105*, 5193.

Through-Bond Interaction via Cyclobutane Relay Orbitals as a Means of Extending Conjugation. Synthesis of Tricyclo[5.5.0.0^{2,8}]dodecatetraene, Tricyclo[5.3.0.0^{2,8}]deca-3,5,9-triene, and 9,10-Dimethylenetricyclo[5.3.0.0^{2,8}]deca-3,5-diene

Jürgen Dressel,[1] Kent L. Chasey, and Leo A. Paquette*

Contribution from the Evans Chemical Laboratories, The Ohio State University, Columbus, Ohio 43210.
Received December 3, 1987. Revised Manuscript Received March 24, 1988

Abstract: The title hydrocarbons have been prepared from dimethyl ε-truxillate. Stepwise belting of a preformed all-trans 1,2,3,4-tetrasubstituted cyclobutane with proper differentiation of the 1,3- and 2,4-positions permits the necessary twofold annulation to be accomplished with relative ease. The efficiency of the syntheses has made available quantities of **8**–**10** sufficiently large for physicochemical study.

As a consequence of pioneering work carried out during the last 20 years by Hoffmann,[2] Simmons,[3] Semmelhack,[4] Heilbronner,[5] Nakajima,[6] and Gleiter,[7] we have come to recognize that two π systems linked perpendicularly by a common tetrahedral carbon atom[8] can exhibit through-space interaction. The magnitude of this phenomenon, termed spiroconjugation, is controlled by the interaction matrix term itself ($\beta_{\text{spiro}}^{\mu\nu} = \langle \pi_A^{\mu}|H|\pi_A^{\nu}\rangle$) and the dependence upon degenerate or at least nearly degenerate basis orbital energies. The manifestations of spiroconjugation are therefore at a maximum when $\beta_{\text{spiro}}^{\mu\nu}$ is large and the π fragments within the system are identical.[7a]

Indeed, spiro[4.4]nonatetraene (**1**) exhibits a splitting of its highest filled (and highest unfilled) diene π (π^*) orbitals amounting to 1.23 eV, as revealed by its UV[4d] and PE spectra.[5c]

---

[1] Fulbright Scholar, 1982–1983; Evans Fellow, 1985–1986.

[2] Hoffmann, R.; Imamura, A.; Zeiss, G. D. *J. Am. Chem. Soc.* **1967**, *89*, 5215.

[3] (a) Simmons, H. E.; Fukunaga, T. *J. Am. Chem. Soc.* **1967**, *89*, 5208. (b) Gordon, M. D.; Fukunaga, T.; Simmons, H. E. *Ibid.* **1976**, *98*, 8401.

[4] (a) Semmelhack, M. F.; Foos, J. S.; Katz, S. *J. Am. Chem. Soc.* **1972**, 94, 8637. (b) Semmelhack, M. F.; DeFranco, R. J. *Ibid.* **1972**, *94*, 8838. (c) Semmelhack, M. F.; DeFranco, R. J.; Margolin, J.; Stock, J. *Ibid.* **1973**, *95*, 426. (d) Semmelhack, M. F.; Foos, J. S.; Katz, S. *Ibid.* **1973**, *95*, 7325.

[5] (a) Boschi, R.; Dreiding, A. S.; Heilbronner, E. *J. Am. Chem. Soc.* **1970**, *92*, 123. (b) Batich, C.; Heilbronner, E.; Semmelhack, M. F. *Helv. Chim. Acta* **1973**, *56*, 2110. (c) Batich, C.; Heilbronner, E.; Rommel, E.; Semmelhack, M. F.; Foos, J. S. *J. Am. Chem. Soc.* **1974**, *96*, 7662.

[6] Tajiri, A.; Nakajima, T. *Tetrahedron* **1971**, *27*, 6089.

[7] (a) Dürr, H.; Gleiter, R. *Angew. Chem., Int. Ed. Engl.* **1978**, *17*, 559. (b) Gleiter, R. *Top. Curr. Chem.* **1979**, *86*, 197.

[8] Model calculations have also been performed on spiro compounds with silicon and phosphorus as central atoms (Böhm, M. C.; Gleiter, R. *J. Chem. Soc., Perkin Trans. II* **1979**, 443). The influence of 3d participation on the ground state is found to be small, in line with experimental work performed so far in this area.[9]

[9] (a) Märkl, G.; Merz, A. *Tetrahedron Lett.* **1969**, 1231. (b) Schweig, A.; Weidner, U.; Hellwinkel, D.; Krapp, W. *Angew. Chem., Int. Ed. Engl.* **1973**, **12**, 310. (c) Shain, A. L.; Ackerman, J. P.; Teague, M. W. *Chem. Phys. Lett.* **1969**, *3*, 550.

0002-7863/88/1510-5479$01.50/0